SLAC – PUB – 4380
August 1987
(T/E)

EXCLUSIVE PRODUCTION OF HEAVY MESONS IN e^+e^- ANNIHILATION*

FARHANG AMIRI†
Stanford Linear Accelerator Center
Stanford University, Stanford, California 94305

AND

CHUENG-RYONG JI
Department of Physics, North Carolina State University,
Raleigh, North Carolina 27695

Abstract

Within the framework of a particular model for meson production, we have performed a perturbative QCD analysis for exclusive pair production of heavy mesons. Analytic calculations of angular distributions for pseudoscalar-pseudoscalar, vector-pseudoscalar and vector-vector mesons are presented. Numerical estimates of the cross section, angular distributions and forward-backward asymmetry for various B, B^*, T and T^* mesons are given at an energy range of 20 GeV to 100 GeV. The forward-backward asymmetry from weak electromagnetic interference is found to be large at TRISTAN energy.

Submitted to *Physical Review D*

* Work supported in part by the Department of Energy, Contracts DE–AC07–76ET10723, DE–AS05–79ER1407 and DE–AC03–76SF00515.

† Permanent address: Department of Physics, Weber State College, Ogden, UT 84408.

1. Introduction

The intermediate vector bosons of the *standard model* will be the subject of intense experimental and theoretical investigations once the e^+e^- colliders at SLAC (SLC), Japan (TRISTAN) and CERN (LEP) start operation. In e^+e^- annihilations, the interaction is mediated by the electromagnetic current (γ) and the weak current (Z°).[1] At typical energies of SLC[2] and LEP[3], i.e., $\sqrt{s} \sim M_Z$, the interaction will be dominated by neutral current through Z° production, while at lower energies ($\sqrt{s} \sim 20$ GeV) the electromagnetic current will dominate and Z° contributions will be negligible. The interesting region of medium energy (e.g., TRISTAN[4] energies) will reveal the interference between weak and electromagnetic interactions.

Among many properties of interest to experimental investigations is the forward-backward asymmetry, A_{FB}, which is a representation of the interference between vector and axial couplings. (See Section 2 for the definition of A_{FB}.) Since the vector coupling of Z° to the electron is close to zero ($\sin^2\theta_W \approx 1/4$), A_{FB} can be considered as a measure of weak-electromagnetic interference in e^+e^- annihilations. In this paper we focus on calculating the angular distributions and forward-backward asymmetry for the exclusive pair production of heavy mesons (mesons with at least one heavy quark c, b, t) within the energy range of 20 GeV to 100 GeV.

Since the momentum transfer q involved in these processes, i.e., exclusive heavy meson pair production, is sufficiently large, they may be treated within the framework of perturbative QCD. Our calculation is based on a particular model for exclusive meson pair production.[5] We include explicit effects associated with the meson bound state by assuming that in the low momentum transfer domain the meson wave function describes a quark-antiquark bound state and, that at large momentum transfer, the momentum dependence of the meson wave function is controlled by the Bethe–Salpeter kernel and thus by single-gluon exchange in the asymptotic limit. The mechanism based on this idea for exclusive production of heavy mesons is shown in Fig. 1. In Figs. 1(a) and 1(b), the process is mediated via photon production while in Figs. 1(c) and 1(d) it is mediated by Z° boson. The main contribution from each set of diagrams depends on the energy regions as will be discussed in Section 3. In this model, the invariant amplitude $\mathcal{M}$ at the large momentum transfer q for processes of Fig. 1 factorizes[5,6] into the convolution of hard scattering amplitude T_H and meson distribution amplitude ϕ_M. The requirement of large momentum transfer q is a necessary condition for factorization[7] of invariant amplitude. Accordingly, the momentum transfer must be larger than the QCD scale parameter $\Lambda \sim 100$ MeV. In Fig. 1, the momentum transfer scale is set up by gluon momentum which is fixed by $\sqrt{s}(1 - m_1/m)$, where m_1 and m are the masses of primary quark and meson, respectively. Therefore, for the heavy meson pair production processes (i.e., $m_1 = m_c, m_b, m_t$) we can invoke the factorization theorem.

To leading order in $1/q^2$, the amplitude for meson pair production is given by the factorized form ($q^2 = s$ in e^+e^- c. m. system)

$$\mathcal{M} = \int [dx_i] \int [dy_j]\, \phi^*_M\left(x_i, \tilde{q}^2\right) T_H\left(x_i, y_j; q^2, \theta_{CM}\right) \phi_M\left(y_j, \tilde{q}^2\right) \quad , \qquad (1)$$

where $[dx_i] = \delta\left(1 - \sum_{k=1}^{n} x_k\right) \prod_{k=1}^{n} dx_k$ and $n = 2$ is the number of quarks in the valence Fock state. The scale $\tilde{q}^2$ is set from higher order calculations, but it reflects the minimum momentum transfer in the process.[5,6] The main dynamical dependence of the form factor is controlled by the hard scattering amplitude T_H which is computed by replacing each hadron by collinear constituents with momenta $x_i p_1$ or $y_i p_2$ where p_1 and p_2 are the momentum of the mesons. Since the collinear divergences are summed in ϕ_M, T_H can be systematically computed by a perturbative expansion in $\alpha_s(q^2)$.[8]

For the heavy quark system,[5] we use the bound state wave function determined by nonrelativistic considerations as a further model assumption. The use of nonrelativistic wave function is probably not realistic, especially for mesons in which the lighter quark mass is comparable to binding energy. It serves, however, as a useful guide and one eventually hopes to use the actual distribution amplitudes when they become available. For now, the use of simplified distribution amplitudes can be thought as applying the mean value theorem to the integral over x with average x taken as an effective mass ratio. For mesons with the spin λ, ϕ_{M_λ} is generically given by[5,6]

$$\phi_{M_\lambda}\left(x_i, q^2\right) = \frac{f_{M_\lambda}}{2\sqrt{3}}\delta\left(x_1 - \frac{m_1}{m}\right) \tag{2}$$

where f_{M_λ} is the decay constant of heavy meson with spin λ such that $f_{M0} = f_{ps}$ (pseudoscalar) and $f_{M1} = f_v$ (vector).

In Section 2, we derive the analytic results for angular distributions of mesons with different spin combinations. Section 3 is devoted to numerical estimates of angular distributions and forward-backward asymmetry, and Section 4 contains a summary of our results and conclusions.

2. Angular Distributions and Asymmetry

The hard scattering part of the amplitude $\mathcal{M}$ in Eq. (1) can be written as a general form given by

$$T_H = -i \sum_{I=\gamma,Z} \left(H^I_\mu(a) + H^I_\mu(b) \right) L^\mu_I \Big/ s_I \tag{3}$$

where $s_\gamma = s$ and $s_Z = s - M_Z^2 + i\Gamma_Z M_Z$. Using the property of δ-function in Eq. (2), the leptonic and hadronic parts of the amplitude are given by

$$L^\mu_I = -i\bar{v}\,(k_2)\,\gamma^\mu\,\Gamma^I_e\,u\,(k_1) \tag{4a}$$

$$\begin{aligned} H^I_\mu(a) = \frac{i4\pi\alpha_s C_F}{s^2(1-r)^3}\, T_r \Bigg\{ &\left[\sum_{\text{spins}} v(rp_2)\bar{u}\left((1-r)\,p_2\right) \right] \cdot \gamma_\alpha \\ &\cdot \left[\sum_{\text{spins}} v\left((1-r)\,p_1\right)\bar{u}(rp_1) \right] \gamma^\alpha \left(\not{q} - r\not{p}_2 + rm \right) \gamma_\mu\,\Gamma^I_Q \Bigg\} \end{aligned} \tag{4b}$$

$$\begin{aligned} H^I_\mu(b) = \frac{i4\pi\alpha_s C_F}{s^2(1-r)^3}\, T_r \Bigg\{ &\left[\sum_{\text{spins}} v(rp_2)\bar{u}\left((1-r)p_2\right) \right] \gamma^\alpha \cdot \\ &\cdot \left[\sum_{\text{spins}} v\left((1-r)p_1\right)\bar{u}(rp_1) \right] \gamma_\mu\,\Gamma^I_Q \left(- \not{q} + r\not{p}_1 + rm \right) \gamma_\alpha \Bigg\} \end{aligned} \tag{4c}$$

where $C_F = 4/3$ is a color factor, $r = m_1/m$, and

$$\begin{aligned} &\Gamma^\gamma_e = e \quad , \quad \Gamma^z_e = V_e + A_e\,\gamma_5 \\ &\Gamma^\gamma_Q = Q_e \quad , \quad \Gamma^z_Q = V_Q + A_Q\,\gamma_5 \\ &V_Q = 2I_3 - 4Q\sin^2\theta_W \quad , \quad V_e = 4\sin^2\theta_W - 1 \\ &A_Q = -2I_3 \quad , \quad A_e = 1 \quad . \end{aligned} \tag{5}$$

Here the spin sum notation $\sum_{\text{spin}}$, includes the appropriate Clebsch–Gordon coefficients for the meson spin wave function.

In Eq. (5), I_3 is the third component of the weak isospin of the quark coupled to Z°, and Q is the charge of the quark (in the unit of e, electron charge).

The spin sums appearing in Eqs. (4b) and (4c) would result in a particular spin combination between produced mesons. For pseudoscalar mesons, the spin sum becomes[6,9]

$$\sum_{\text{spin}} v(rp_2)\bar{u}\left((1-r)p_2\right) = \frac{\gamma_5(\not{p}_2 + m)}{\sqrt{2}} \quad . \tag{6}$$

While for vector mesons

$$\sum_{\text{spins}} v(rp_2)\bar{u}\left((1-r)p_2\right) = \frac{\not{\epsilon}(\not{p}_2 + m)}{\sqrt{2}} \quad . \tag{7}$$

The differential cross section can be written in terms of amplitude $\mathcal{M}$ as

$$\frac{d\sigma}{d\cos\theta} = \frac{\overline{|\mathcal{M}|}^2}{32\pi s}\sqrt{1-\tau^2} \tag{8}$$

where $\tau^2 \equiv 4m^2/s$. Using Eqs. (2)–(8), the angular distribution for a particular spin combination of produced mesons becomes

$$\begin{aligned}\left(\frac{d\sigma}{d\cos\theta}\right)_{e^+e^-\to M_\lambda M_{\lambda'}} &= \frac{\pi^3\, f^2_{M\lambda} f^2_{M\lambda'}\, \sqrt{1-\tau^2}\cdot\alpha^2\cdot\alpha_s^2}{81(1-r)^6\sin^4 2\theta_W\, s\left\{(s-M_Z^2)^2+\Gamma_Z^2 M_Z^2\right\}} \\ &\quad \cdot\left[c_1^{\lambda\lambda'}\sin^2\theta + c_2^{\lambda\lambda'}(1+\cos^2\theta) + c_3^{\lambda\lambda'}\cos\theta\right]\end{aligned} \tag{9}$$

where λ and λ' refer to helicity states of the mesons, and coefficients $c_i^{\lambda\lambda'}$ are given in Table 1.

The calculation of asymmetry can proceed along the same lines. By definition, A_{FB} is

$$A_{FB} \equiv \frac{\int_0^1 \left(\frac{d\sigma}{d\cos\theta}\right) d\cos\theta - \int_{-1}^0 \left(\frac{d\sigma}{d\cos\theta}\right) d\cos\theta}{\sigma} \quad , \tag{10}$$

where σ is the total cross section. Substituting for $d\sigma/d\cos\theta$ from Eq. (9), the asymmetry becomes,

$$A_{FB}^{\lambda\lambda'} = \frac{3c_3^{\lambda\lambda'}}{4c_1^{\lambda\lambda'} + 8c_2^{\lambda\lambda'}} \tag{11}$$

with the coefficients $c_i^{\lambda\lambda'}$ as given in Table 1. The numerical estimates of the angular distribution and A_{FB} for different mesons will be presented in the next section. At this point, however, we need to make a few comments with regard to the meson decay constants as introduced in Eq. (2). Due to uncertainties in parameters such as f_{ps} and f_v, it is rather difficult to predict how much smaller the cross section of exclusive process is than that of the corresponding inclusive process. If we use the present parameters as given in Table 2, however, then we have a factor between 10^{-2} - 10^{-3} compared to inclusive processes.[10] There is a large range of variations for the numerical values of some meson decay constants. For exclusive reactions we are considering, this can introduce about an order of magnitude uncertainty in the estimates of cross sections. More detail will be given in the next section.

3. Numerical Estimates

i) $e^+e^- \to ps + \overline{ps}$ $(\lambda = \lambda' = 0)$

For two pseudoscalar mesons, the interference between axial and vector coupling terms vanishes. As a result, the angular distribution $d\sigma/d\cos\theta$ is symmetric. It is dominated by γ-exchange at lower energies ($s \ll M_Z^2$) and by Z°-exchange at higher energies ($s \approx M_Z^2$). A particularly striking feature of the present QCD model predictions is the existence of a zero in e^+e^- annihilation cross section for pseudoscalar meson pair production at the specific timelike value $\sqrt{s} = \sqrt{2r/(1-r)}m$ (see Table 1). The existence of a zero in the form factor and e^+e^- annihilation cross section for a pair of spin-zero mesons was first predicted in Ref. 5 for pure electromagnetic processes. By including Z° contributions, however, the same phenomena still exist. In Fig. 2, the angular distributions for production of $B_u\overline{B}_u$ mesons are shown [see Eq. (9)] where the numerical values of masses and decay constants are taken from Table 2. As we can see the normalization of angular distribution becomes exceedingly small as $\sqrt{s}$ is close to $\sqrt{2r/(1-r)}m \approx 31$ GeV.

ii) $e^+e^- \to ps + V$ $(\lambda = 1\ ,\ \lambda' = 0)$

In this case, as observed from Table 1, the coefficient $c_3^{10} \neq 0$ which gives rise to a finite asymmetry, A_{FB}. Again, for $s \ll M_Z^2$, the EM current dominates; interference term will be small and angular distribution is rather symmetric. At medium energies, however, γ-Z° interference becomes large which result in an asymmetrical angular distribution. These features can also be deduced from the analytic expression derived for angular distribution $d\sigma/d\cos\theta$ in Section 2. From Eq. (9) and Table 1 we observe that due to factor $(1 - r)^2$ in c_1^{10}, this coefficient is small compared to c_2^{10} and c_3^{10} and, consequently, the terms proportional to $(1+\cos^2\theta)$ and $\cos\theta$ are the main contributions to $d\sigma/d\cos\theta$. For $s \ll M_Z^2$, it can be easily seen that $c_2^{10} \gg c_3^{10}$ and a symmetric angular distribution will result. On the other hand, for $\sqrt{s} \approx M_Z/2$, the coefficient c_3^{10} will dominate and the

$\cos\theta$ term in Eq. (9) determines the shape of angular distribution. At $s \approx M_Z^2$, the interference between γ and Z° disappears due to negligible contribution from γ-exchange. Nevertheless, the cross terms arising from V–A interference in the Z°-couplings to quarks and leptons give rise to an asymmetry and c_3^{10} still remains larger than c_2^{10}. These features are shown in Fig. 3 where we have plotted the angular distributions for B_u-mesons at various energies. The forward-backward asymmetry A_{FB}, which is given by Eq. (11) and plotted in Fig. 4 indicates the intersecting region of TRISTAN energy range for B_u-mesons. For T–meson production the available phase space is very limited due to the heavy mass of t-quark. As shown in Figs. 5 and 6, however, many features of electroweak symmetry breaking can be tested around the energy range of SLC and LEP.

iii) $e^+e^- \to V + V$ $(\lambda = \lambda' = 1)$

At energies close to threshold, angular momentum conservation dictates an angular distribution dominated by terms proportional to $\sin^2\theta$, if r is not close to 1 (e.g., B_u production). At this energy Z° effect will be negligible and coefficient c_1^{11} is much greater than c_2^{11} and c_3^{11} in Eq. (9). This feature is clearly exhibited in Fig. 7(a) where the angular distribution of a pair of B_u-mesons is plotted at an energy close to threshold. As the energy increases, the related orbital angular momentum can assume different values, and all of terms in Eq. (9) contribute to angular distribution (see Fig. 7). At energies $\sqrt{s} \approx M_Z/2$, the γ-Z° interference becomes large compared to other contributions and a very asymmetric distribution will result. As discussed for (V+ps) production, near Z°-pole, the γ effect is negligible and only a slight asymmetry arises from V–A cross terms in the Z°-couplings to quarks and leptons. The forward-backward asymmetry shown in Figs. 4 and 6 (dashed line) have very similar features to the case of (V+ps) production discussed in the preceding part.

4. Summary and Conclusions

Studying heavy meson production processes at e^+e^- colliders like TRISTAN, SLC and LEP can provide valuable information about: a) QCD mechanism responsible for hadroniziation of heavy quarks to heavy mesons and b) electroweak couplings of Z° to quarks and leptons.

For the case of exclusive production of heavy mesons, we presented the angular distributions for pseudoscalar and vector mesons. The onset of leading power behavior is controlled simply by the mass parameters of the theory. Specifically, we confirmed that the present model based on perturbative QCD predicts a zero[5] in the cross section for the exclusive pseudoscalar meson pair production even after weak interactions are incorporated into the model by including Z°-production. Although the cross sections for exclusive processes are small compared to single particle inclusive reactions[10] and require large luminosity, the observation of zero cross section by the present model can provide a unique test of the theory and its applicability to exclusive processes.

We also found that γ-Z° interference effects give rise to a rather large forward-backward asymmetry when a vector meson is produced. Specifically, for vector mesons production, the shape of angular distribution, $1 + \alpha\cos^2\theta + \beta\cos\theta$ changes from $\alpha = -1$ and $\beta = 0$ near threshold to $\alpha > 0$ and $\beta \neq 0$ away from the threshold (see Fig. 7). These effects become small near Z°-pole; however, for $\sqrt{s} = M_Z$ (where the cross section is rather large), there is still slight asymmetry which is solely due to V–A interference in the Z° coupling to quarks and leptons. Finally, the forward-backward asymmetry from weak and electromagnetic interference is found to be large within the TRISTAN energy range.

References

1. For a review, see C. Quigg, *Gauge Theories of Strong, Weak, and Electromagnetic Interactions* (Benjamin, New York, 1983).
2. Proceedings of the Stanford Linear Collider User Meeting, Stanford, California, 1981 (SLAC Report No. 247, 1982).
3. *Physics at LEP,* Proceedings of the LEP Physics Jamboree, edited by John Ellis and Roberto Peccei (CERN Report No. 86–02, 1986).
4. Proceedings of the Second TRISTAN Physics Workshop, Ed. Y. Unno, KEK 82–1 (1982).
5. The same model was used for the exclusive heavy meson production without including the Z°-boson contribution by S. J. Brodsky and C. R. Ji, Phys. Rev. Lett **55,** 2257 (1985).
6. G. P. Lepage and S. J. Brodsky, Phys. Rev. **D22,** 2157 (1980); F. Amiri, B. C. Harms and C. R. Ji, Phys. Rev. **D32,** 2982 (1985).
7. For a recent review of factorization theorems of perturbative QCD, see J. C. Collins and D. E. Soper, OITS350 preprint (1987), submitted to Annual Review of Nuclear and Particle Science.
8. G. P. Lepage, S. J. Brodsky, T. Huang and P. B. Mackenzie, CLNA–82/522 (1982), published in the Proceedings of the Banff Summer Institute on Particles and Fields, edited by A. Capri and A. N. Kamal, Plenum Press (1982).
9. E. L. Berger and D. Jones, Phys. Rev. **D23,** 1521 (1981).
10. For an analysis of inclusive heavy meson production based on present model, see C. R. Ji and F. Amiri, Phys. Rev. **D23,** 3318 (1987) and F. Amiri and C. R. Ji, Phys. Lett. B (to be published).

Table 1

Coefficients $c_i^{\lambda\lambda'}$ in Eqs. (9) and (11). Note that $V_{Qe} = V_Q V_e - 4Q \sin^2 2\theta_W [(s - M_Z^2)/s]$.

$\lambda\lambda'$ \ $c_i^{\lambda\lambda'}$	$c_1^{\lambda\lambda'}$	$c_2^{\lambda\lambda'}$	$c_3^{\lambda\lambda'}$
0,0	$(1-\tau^2)\{2(1-r) - r\tau^2\}^2 \cdot (V_{Qe}^2 + A_e^2 V_Q^2)$	0	0
0,1 1,0	$4(1-r)^2 A_Q^2 (V_e^2 + A_e^2)$	$\tau^2[(1-\tau^2)(V_{Qe}^2 + V_Q^2 A_e^2) + \{(2-r)^2 + r\tau^2(r\tau^2 + 2r - 4)\} \cdot A_Q^2 (V_e^2 + A_e^2)]$	$4\tau^2(1-\tau^2)^{1/2}(2 - r - r\tau^2) \cdot A_Q A_e (V_{Qe} + V_Q V_e)$
1,1	$2(1-\tau^2)\{2(1-r)^2 + 2r(1-r)\tau^2 + 3/2 r^2 \tau^4\}(V_{Qe}^2 + A_e^2 V_Q^2)$	$2\tau^2(1-\tau^2)\{(V_{Qe}^2 + V_Q^2 A_e^2) + (1-\tau^2) \cdot r^2 A_Q^2 (V_e^2 + A_e^2)\}$	$8\tau^2(1-\tau^2)^{3/2} r \cdot A_e A_Q (V_{Qe} + V_e V_Q)$

Table 2

The numerical values of the parameters used in Eqs. (9) and (11).

$\alpha_s = 0.2$	$f_M = 0.28$ GeV	$\Gamma_Z = 2.9$ GeV
$m_t = 40$ GeV	$m_b = 5$ GeV	$m_c = 1.5$ GeV
$m_u = 0.3$ GeV	$M_Z = 92.9$ GeV	$\sin^2\theta_W = 0.23$

Figure Captions

Fig. 1. Exclusive production of mesons in e^+e^- annihilations. Four more diagrams are obtained by exchanging the primary- and secondary-quark pairs.

Fig. 2. Angular distributions for production of $B_u\overline{B}_u$ pseudoscalar mesons.

Fig. 3. Angular distributions for B_u-meson in ($e^+e^- \rightarrow$ ps+V) at various energies.

Fig. 4. Forward-backward asymmetry for B_u-mesons in $e^+e^- \rightarrow$ ps+V (solid line) and $e^+e^- \rightarrow$ V+V (dashed line).

Fig. 5. Angular distributions for T_c-mesons in ($e^+e^- \rightarrow$ ps+V) at various energies.

Fig. 6. Forward-backward asymmetry for T_c-mesons in $e^+e^- \rightarrow$ ps+V (solid line) and $e^+e^- \rightarrow$ V+V (dashed line).

Fig. 7. Angular distributions for B_u^*-mesons in ($e^+e^- \rightarrow$ V+V) at various energies.

Fig. 8. Angular distributions for T_c^*-mesons in ($e^+e^- \rightarrow$ V+V) at various energies.

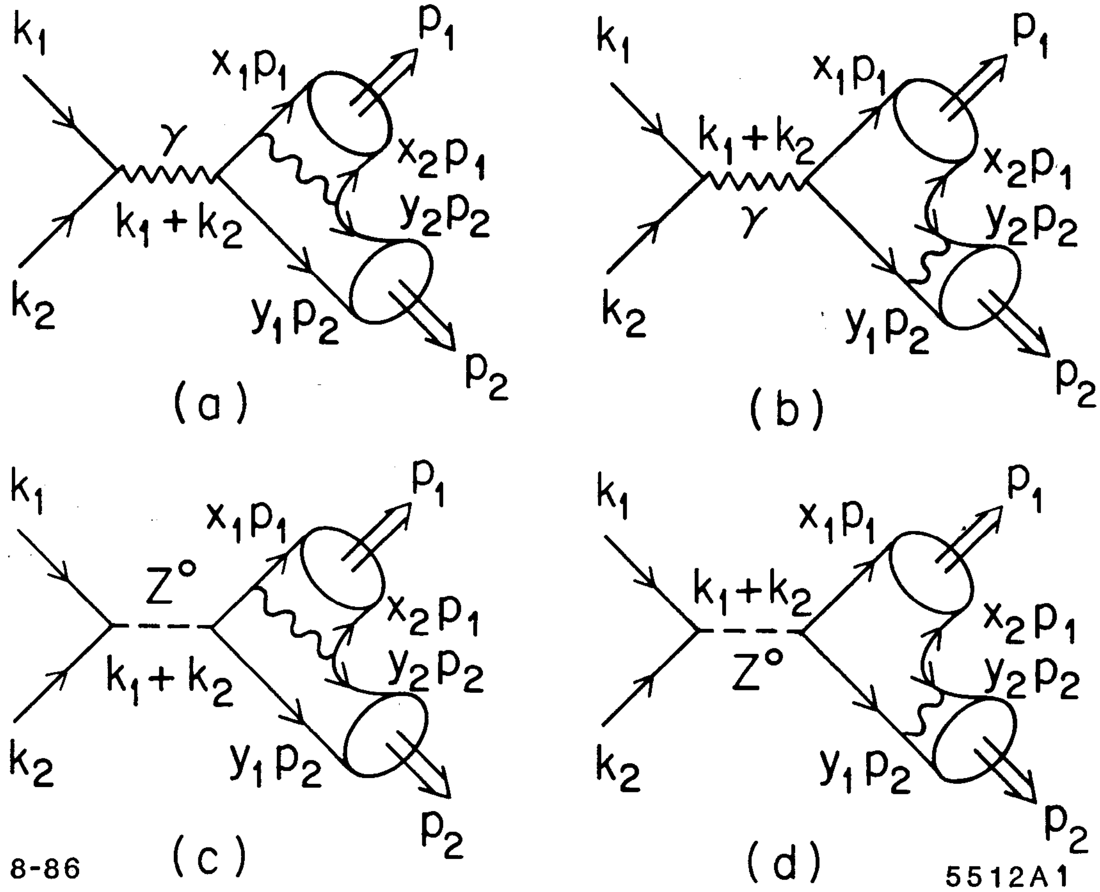

k1
k2
γ
k1 + k2
x1p1
p1
x2p1
y2p2
y1p2
p2
(a)
k1
k2
k1 + k2
γ
x1p1
p1
x2p1
y2p2
y1p2
p2
(b)
k1
k2
Z°
k1 + k2
x1p1
p1
x2p1
y2p2
y1p2
p2
(c)
k1
k2
k1 + k2
Z°
x1p1
p1
x2p1
y2p2
y1p2
p2
(d)
8-86
5512A1

Fig. 1

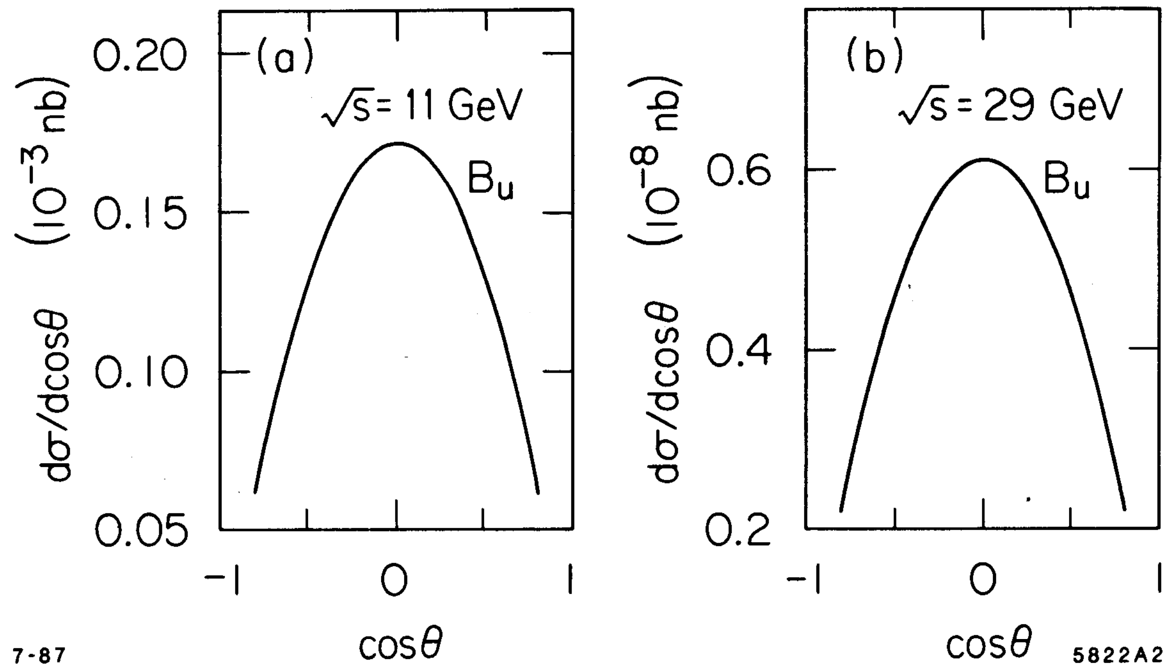

(a)
$\sqrt{s}$ = 11 GeV
B_u
0.20
0.15
0.10
0.05
dσ/dcosθ (10⁻³ nb)
−1
0
1
cosθ
7-87
(b)
$\sqrt{s}$ = 29 GeV
B_u
0.6
0.4
0.2
dσ/dcosθ (10⁻⁸ nb)
−1
0
1
cosθ
5822A2

Fig. 2

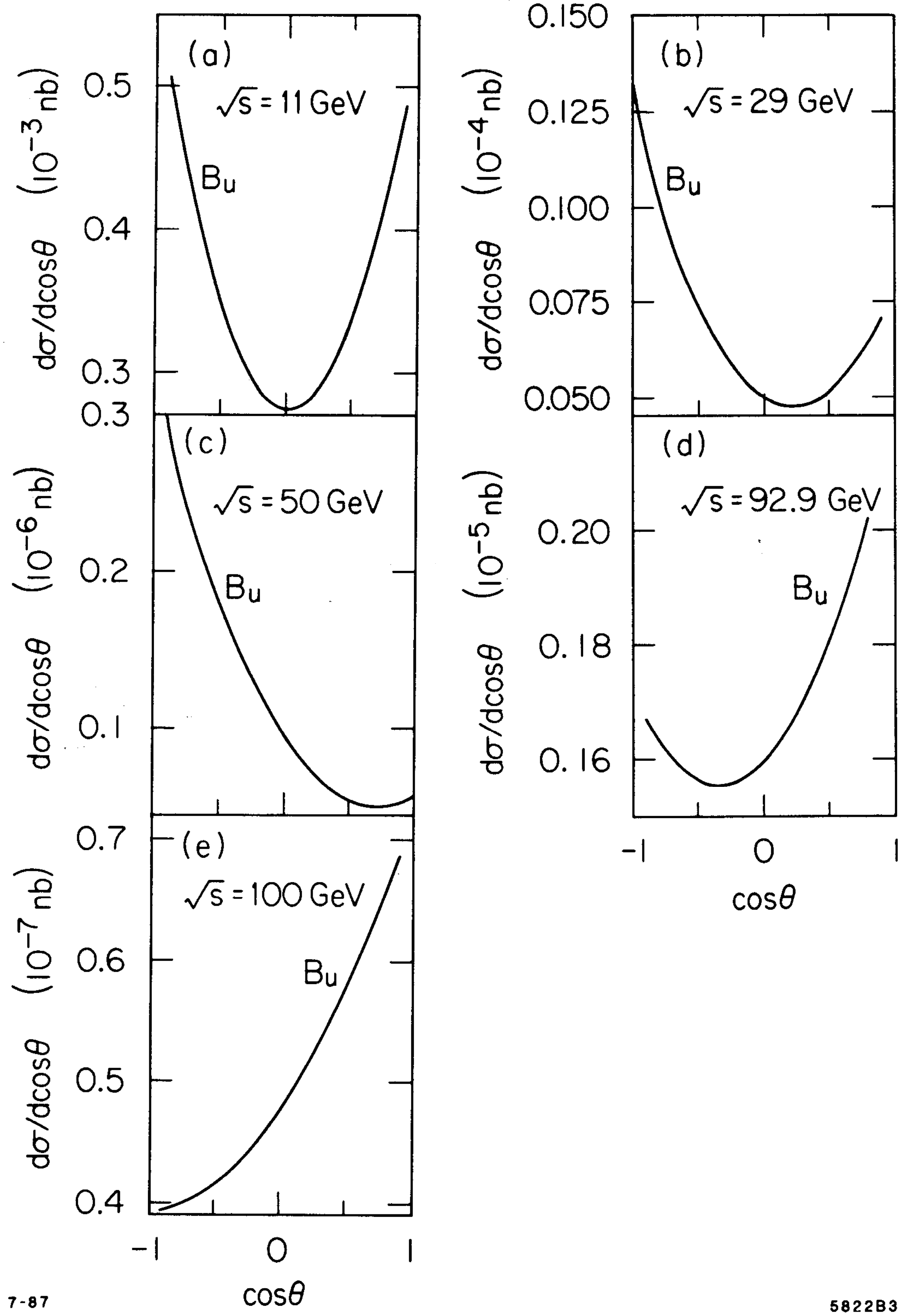

(a)
$\sqrt{s}$ = 11 GeV
B_u
$d\sigma/d\cos\theta$ $(10^{-3}$ nb)
0.5
0.4
0.3
(b)
$\sqrt{s}$ = 29 GeV
B_u
$d\sigma/d\cos\theta$ $(10^{-4}$ nb)
0.150
0.125
0.100
0.075
0.050
(c)
$\sqrt{s}$ = 50 GeV
B_u
$d\sigma/d\cos\theta$ $(10^{-6}$ nb)
0.3
0.2
0.1
(d)
$\sqrt{s}$ = 92.9 GeV
B_u
$d\sigma/d\cos\theta$ $(10^{-5}$ nb)
0.20
0.18
0.16
(e)
$\sqrt{s}$ = 100 GeV
B_u
$d\sigma/d\cos\theta$ $(10^{-7}$ nb)
0.7
0.6
0.5
0.4
-1
0
1
$\cos\theta$
7-87
5822B3

Fig. 3

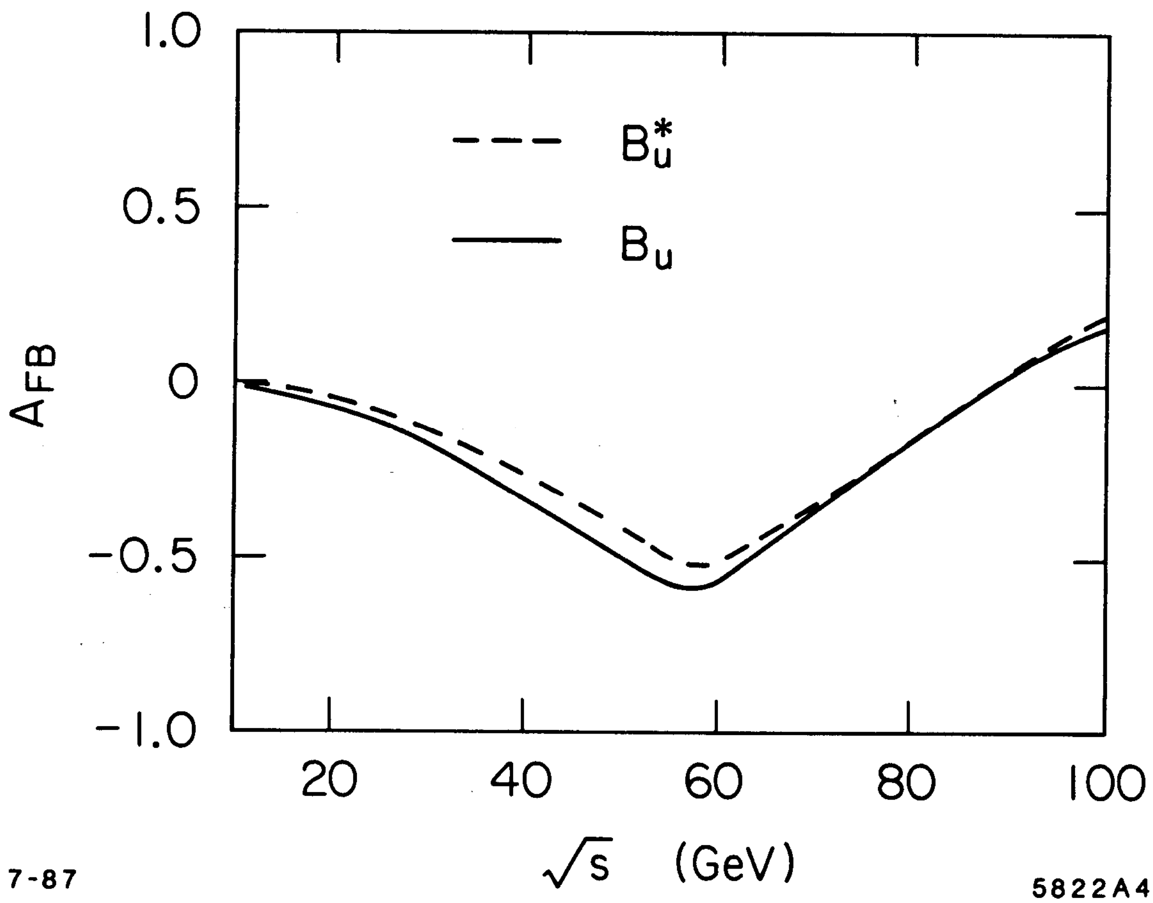

Fig. 4

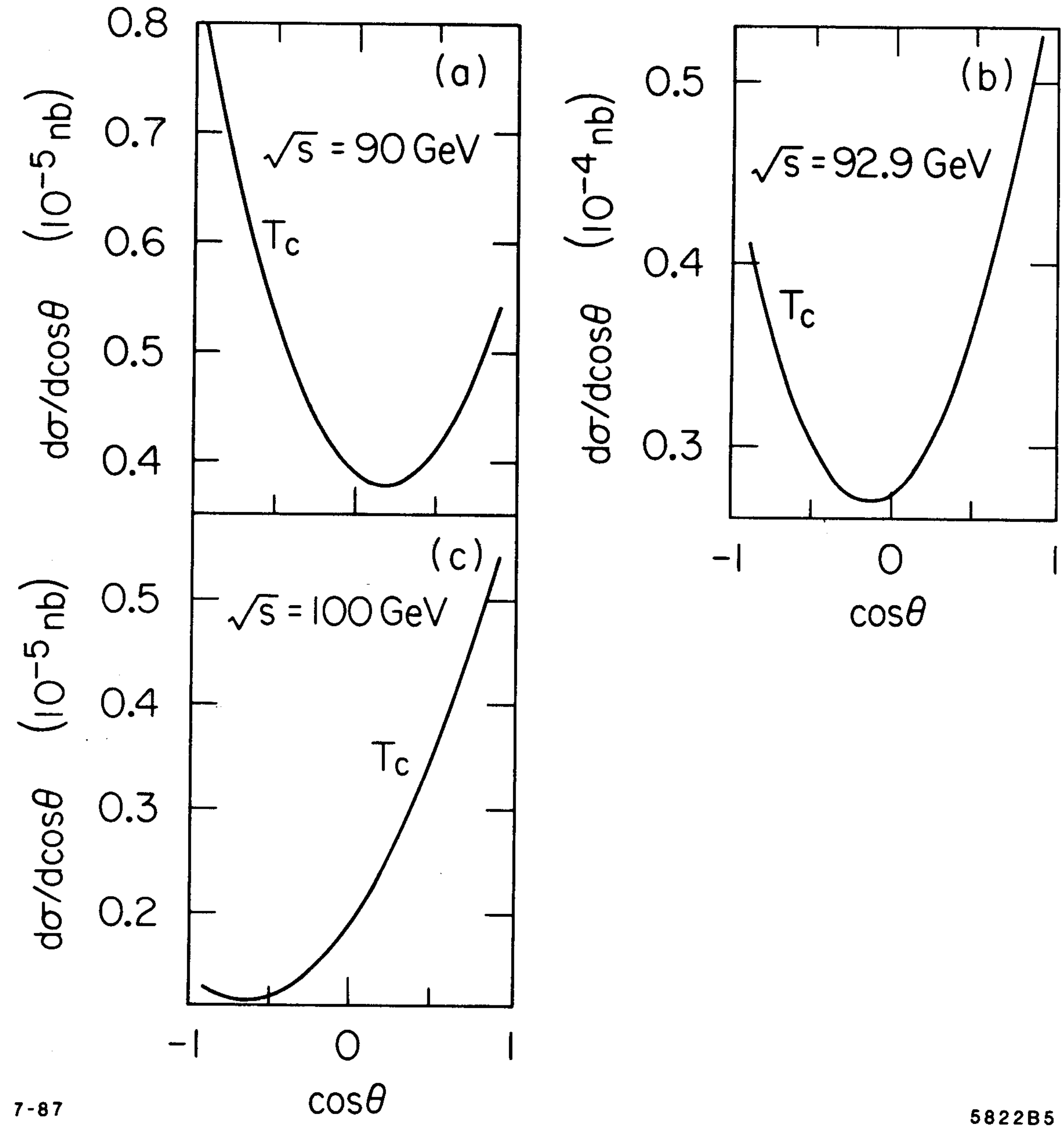
(a)
$\sqrt{s}$ = 90 GeV
T_c
(b)
$\sqrt{s}$ = 92.9 GeV
T_c
(c)
$\sqrt{s}$ = 100 GeV
T_c
$d\sigma/d\cos\theta$ $(10^{-5}$ nb)
$d\sigma/d\cos\theta$ $(10^{-4}$ nb)
$d\sigma/d\cos\theta$ $(10^{-5}$ nb)
0.8
0.7
0.6
0.5
0.4
0.5
0.4
0.3
0.5
0.4
0.3
0.2
-1
0
1
$\cos\theta$
7-87
5822B5

Fig. 5

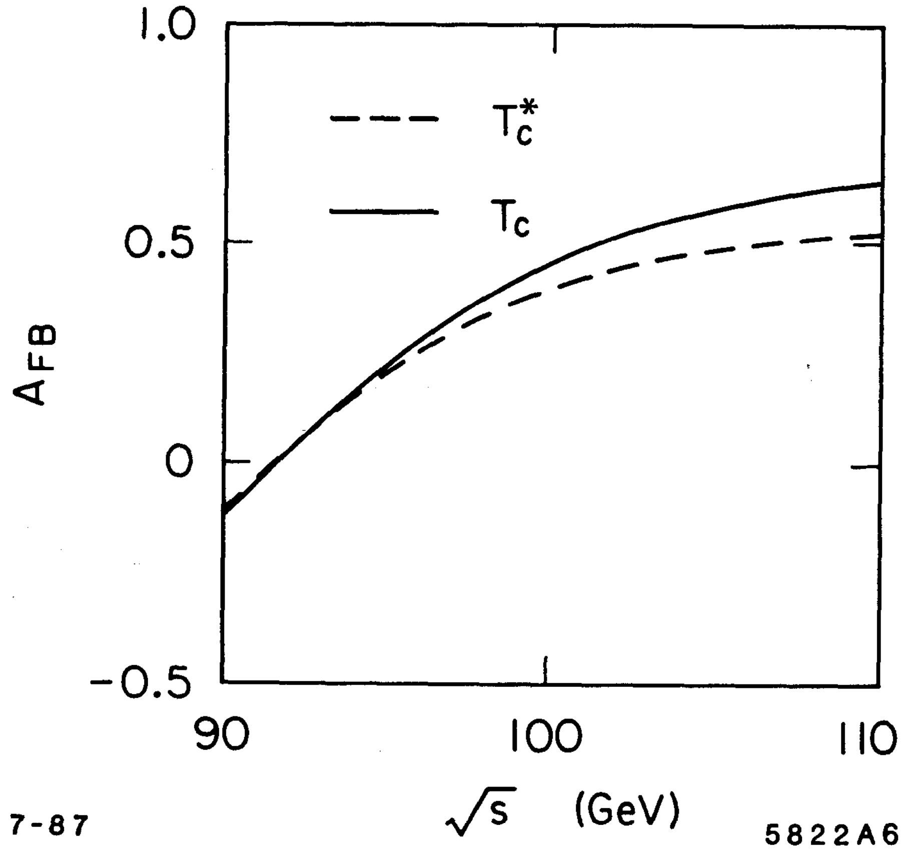

Fig. 6

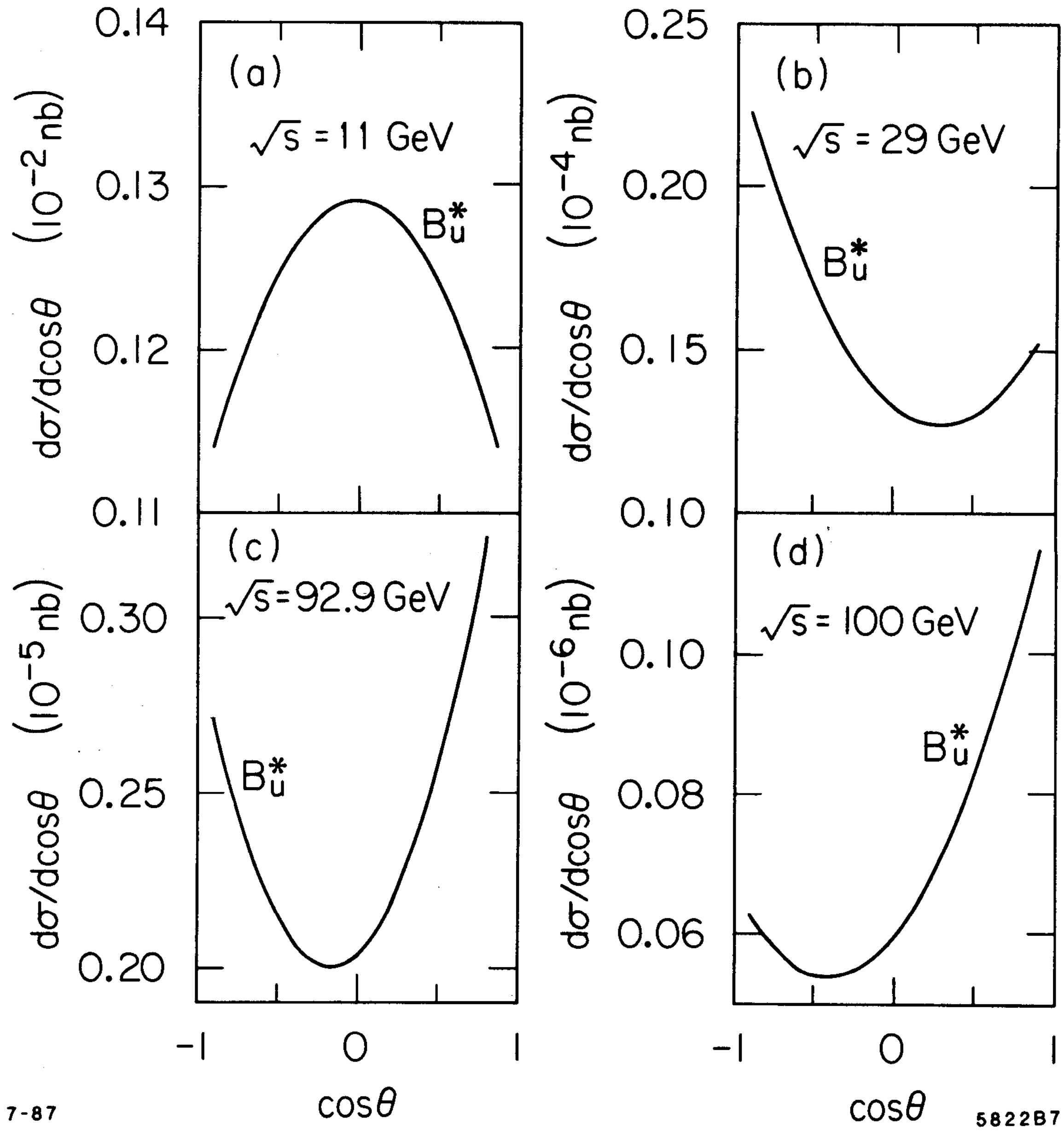

(a)
$\sqrt{s}$ = 11 GeV
B_u^*
(b)
$\sqrt{s}$ = 29 GeV
B_u^*
(c)
$\sqrt{s}$=92.9 GeV
B_u^*
(d)
$\sqrt{s}$= 100 GeV
B_u^*
$d\sigma/d\cos\theta$ $(10^{-2}$nb)
$d\sigma/d\cos\theta$ $(10^{-4}$nb)
$d\sigma/d\cos\theta$ $(10^{-5}$nb)
$d\sigma/d\cos\theta$ $(10^{-6}$nb)
0.14
0.13
0.12
0.11
0.25
0.20
0.15
0.10
0.30
0.25
0.20
0.10
0.08
0.06
-1
0
1
$\cos\theta$
7-87
5822B7

Fig. 7

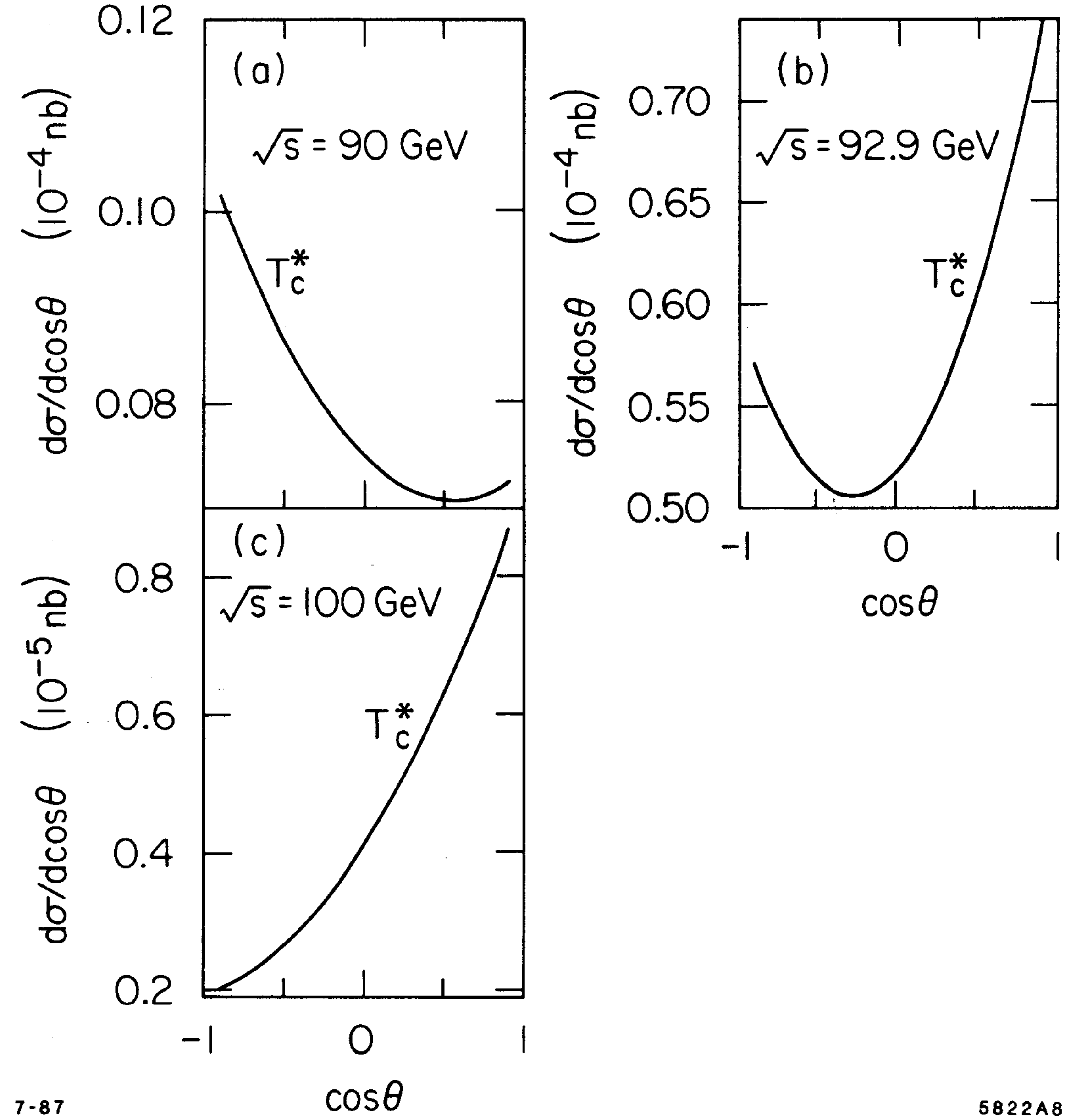

7-87

5822A8

Fig. 8